Comparative Medicine
Copyright 2017
by the American Association for Laboratory Animal Science

Vol 67, No 5
October 2017
Pages 388–399

Original Research

Effect of Early-life Gut Mucosal Compromise on Disease Progression in NOD Mice

Katja M Bendtsen,[1,*] Camilla HF Hansen,[1] Lukasz Krych,[3] Karsten Buschard,[2] Helene Farlov,[1] and Axel K Hansen[1]

Disease expression in spontaneous nonobese diabetic (NOD) mice depends on environmental stimuli such as stress, diet, and gut microbiota composition. We evaluated a brief, early-life gut intervention in which pups were weaned to low-dose dextran sulfate sodium (DSS). We hypothesized that the mucus-reducing effect of this compound and subsequent increased host–bacterial contact would delay disease onset and decrease insulitis due to enhanced oral tolerance. However, disease incidence did not differ between groups, although median survival (time point when 50% of the mice are still alive) of the control group was 184 d compared with 205 d for DSS-treated mice. Mean age at disease onset (that is, blood glucose of at least 12 mmol/L) was 164 d for control mice and 159 d for DSS-treated mice. In addition, 62.5% of control mice reached a blood glucose of 12 mmol/L before 30 wk of age compared with 59% in DSS-treated mice, which had a significant transient increase in serum insulin in week 4. No changes were found in immune cells collected from spleen, pancreatic lymph nodes, and mesenteric lymph nodes. Although mice received a low dose of DSS, the subsequent reduction in the diversity of the microbiota during weeks 4 through 6 led to increased cecal length and weight and, in week 13, a tendency toward decreased colon length, with increased leakage of LPS to the blood. We conclude that mucus reduction and subsequent increased host–bacterial contact did not affect overall disease progression in NOD mice.

Abbreviations: DSS: dextran sulfate sodium; NOD, nonobese diabetic; OTU, operational taxonomic unit; T_{reg}, regulatory T cells

The nonobese diabetic (NOD) mouse is an extensively studied spontaneous genetic model for the development of type 1 diabetes mellitus. This immune-mediated disease is caused by molecular dysfunction leading to the rise of islet-antigen–specific cells, which autonomously attack the insulin-producing β cells in the pancreas. The insulitis is of a mixed and progressive nature, with infiltration innately initiated by neutrophils, dendritic cells, and macrophages and continued through both T and B lymphocyte reactivity.[11,29] Typically NOD mice are diagnosed when blood glucose reaches 12 mmol/L (reference value, 4 to 6 mmol/L) beginning at approximately 10 wk of age, however prediabetic mechanisms are recognizable from as early as 3 to 6 wk.[7,11] Despite the strong genetic and molecular background, the model is further complicated in its etiology by many external manipulations that affect disease outcome. In addition to a sex-associated bias, with an incidence of 40% to 90% in females compared with 10% to 40% in males,[11] the incidence, progression, and severity of the hyperglycemia in NOD mice are dependent on environmental circumstances from fetus to adult. Housing, handling, and transportation stress have often been claimed to alter incidence, likely mediated through stress-related changes in the gut microbiota.[2,30] Gluten in the diet is known as a strong trigger; NOD mothers kept on a gluten-free diet give birth to low incidence pups, and similar results are achieved in weaning the pups from a standard fed mother to a gluten-free diet.[16,21] The effect is in fact considered to be mediated by the microbiota of the gut, which has an important influence on the onset and progression in this model,[19,26] as with other inflammatory diseases due to the effect on regulatory immune priming.[3] The importance of mucosal immune interaction with commensal bacteria and indigenous antigens for tolerance maintenance is shown in several studies,[1,9,15,23] and enhancing the regulatory immune environment in this model was previously reported as a suggested factor in disease amelioration.[6,10,17,19] Even though no translational treatments have yet been achieved, the NOD mouse model has great value in search for basic mechanistic understanding exploitable in human diabetes research. In fact, a gluten-free diet is a promising prevention in maintaining children off insulin treatment.[32]

Because 'diabetogenic' microbiota compositions have been proposed,[5] factors that influence the gut microbiota composition in NOD mice should be assessed. For example, a change from neutral to acidified water decreased diabetes incidence, with a shift to decreased Firmicutes and increased Bacteriodetes, Actinobacteria, and Proterobacteria and upregulation of Th17 and regulatory T cells (T_{reg}).[34] In the current study, we weaned NOD pups to drinking water supplemented with a low dose of dextran sulfate sodium (DSS), which compromises the gut barrier; higher concentrations of DSS (usually 3% to 5%) cause colitis in rodents, depending on strain, duration, and concentration.[18,28]We have previously shown that low-dose DSS treatment compromises the gut barrier due to an acute regulatory immunologic response influenced by dietary antigens and that DSS treatment changes the

Received: 30 May 2016. Revision requested: 09 Aug 2016. Accepted: 08 Jan 2017.
[1]Section of Experimental Animal Models, Department of Veterinary Disease Biology, Faculty of Health and Medical Sciences, University of Copenhagen, Frederiksberg, Denmark; [2]The Bartholin Institute, Copenhagen, Denmark; and [3]Department of Food Science, Faculty of Life Sciences, University of Copenhagen, Frederiksberg, Denmark.
**Corresponding author: kab@sund.ku.dk*

composition of gut microbiota toward decreased gram-positive and increased gram-negative species,[4] which findings best are in line with other studies. [12,31] Knowing the relevance of both the gut microbiota and regulatory functions, we chose the NOD model to evaluate the hypothesis that brief gut mucosal compromise during early life would delay disease onset and decrease insulitis due to increased host–microbial contact and increased stimulation of T_{reg} cells, thereby testing the robustness of the model.

Materials and Methods

This study was in agreement with the Directive 2010/63/EU of the European Parliament, the Council of 22 September 2010 on the protection of animals used for scientific purposes, and the Danish Animal Experimentation Act (LBK 474 15/05/2014). The study was approved by the Animal Experiments Inspectorate under the Ministry of Environment and Food in Denmark (license no. 2012-15-2934-00256 C1-5).

Mice. All animals were female NOD/BomTac mice, bred onsite in barrier-protected rooms, and weaned at 3 wk (minimal body weight, 6.5 g). The breeding mice were purchased from Taconic (Hudson, NY) and were free of murine pathogens evaluated during their routine health monitoring program. At our facility, sentinel mice were serologically tested for and found free of mouse hepatitis virus, reovirus type 3, Theiler virus (GDVII), Sendai virus, minute virus of mice, mouse parvovirus, rotavirus (EDIM), and *Clostridium piliforme* (Biodoc Diagnostics, Hannover, Germany). Fecal samples from cages were tested inhouse for endoparasites (Fecalyzer, Kruuse A/S, Marbjerg, Denmark). Full microbiota 16S sequencing (Miseq, Illumina, San Diego, CA) was done inhouse on samples from all mice from the study. None of the assays revealed any reportable agents according to FELASA guidelines for health monitoring.[14]

The animals were housed in standard cages (type 1290, Techniplast, Buggiatate, Italy) with aspen chip bedding (Tapvei, Harjumaa, Estonia) supplemented with Enviro-Dri and Alpha-Nest nesting material (Shepard Specialty Papers, Watertown, TN), Shepherd Shacks (Shepard Specialty Papers), and an aspen chew block (Tapvei). They were fed a standard diet (no. 1324, Altromin, Lage, Germany) and housed under a 12:12-h light:dark cycle (lights on, 0700) with 55% humidity and temperature of 20 to 24 °C. Treatment with 1% DSS (molecular weight, 36,000 to 50,000 Da; lot no. M2709; catalog no. 160110, MP Biomedicals, Santa Ana) in free-choice municipal drinking water beginning on the day of weaning, for a total of 7 d. The solution was changed once. Water and food intakes were measured during the treatment week and for 2 wk after.

Design. Two experimental groups of mice were evaluated: an incidence group and a sample-collection group. Untreated control (n = 25) and DSS-treated (n = 29) NOD mice were followed until they were 30 wk old. The mice were weighed and cage-changed once weekly and handled minimally. From week 10 through 30, the blood glucose level was measured once each week; if it was at least 7 mmol, the mouse was measured again after 2 d. When the blood glucose level exceeded 12 mmol, the mouse was considered diabetic and euthanized. One control mouse was euthanized early in the study due to a study-unrelated pathogenic finding identified during daily inspection. In addition, 9 control mice (37.5%) and 11 DSS-treated animals (37.9%) did not reach the diabetic threshold of 12 mmol/L.

Of the sample-collection group, 6 control mice and 6 DSS-treated mice were euthanized after the last treatment day (age, 4 wk), and relevant samples collected to evaluate their status. At 6 and 13 wk of age (reflecting early prediabetic state and after normal onset-age, respectively), 8 control and 8 or 9 DSS-treated mice were euthanized, and serum, plasma, feces, cecal contents, weight and length of cecum, length of colon, pancreas, spleen, and pancreatic and mesenteric lymph nodes were collected.

General sampling procedure. The blood glucose was measured by tail sampling (FreeStyle Lite Blood Glucose Monitoring System, Abbott, Chicago, IL), the mouse weighed and then sedated with fentanyl, fluanisone (0.315 mg/mL fentanyl with 10 mg/mL fluanisone, VetPharm, Anglesey, Wales), and 5 mg/mL midazolam (Roche, Denmark) diluted 1:1:2 in sterile water and dosed at approximately 0.6 mL/100 g body weight. Blood was collected from the infraorbital sinus by using a hematocrit tube, first into an EDTA tube and then into a sterile microfuge tube. The EDTA tube was placed on ice, and both tubes were allowed 15 min to coagulate. After centrifugation, plasma and serum were frozen immediately at –20 °C and stored at –80 °C when prolonged reservation was necessary. Immediately after blood collection, the mouse was killed by cervical dislocation. First, the pancreatic lymph nodes were dissected and placed in cold PBS (Sigma–Aldrich, St Louis, MO). Then the pancreas was placed in formaldehyde, and finally the spleen and mesenteric lymph nodes were placed in cold PBS. The gut was exteriorized, the colon and cecum measured, and feces or cecal contents (or both) were collected and frozen immediately at –20 °C and stored at –80 °C when prolonged preservation was necessary.

Flow cytometry. Samples were stored in 1 mL cold PBS (Sigma–Aldrich) in microfuge tubes and processed within 2 h. The cells were isolated by placing the tissue between 2 microscope slides and gently pressing them together. Cells were resuspended in 5 mL PBS, with subsequent filtering through a 100-µm cell strainer (catalog no. 340611, BD Biosciences, San Jose, CA). Lysis, washing, and staining were performed according to the manufacturer's protocol for FoxP3 staining buffer (catalog no. 00-5523-00, eBioscience, San Diego, CA). The following antibodies were used: CD8–APC (catalog no. 561093), CD25–PE (550082), CD4–PerCP (550954), CD25–APC (561048), and CD4–FITC (553046; all from BD Biosciences) and CD3–FITC (11-0032-82), γδ-TCR–PE (12-5711-82), and FOXP3–PE (12-5773-82) from eBioscience. Isotype controls were APC IgG2a (catalog no. 560720), APC IgG1 (554686), and FITC IgG2b (556923) from BD Biosciences and PE IgG1 (12-4301-81) from eBioscience. Flow cytometry was performed by using a model C6 flow cytometer (Accuri Cytometers, Ann Arbor, MI).

Insulin and LPS. Plasma insulin content was measured in duplicate without dilution by using a standard fluorescence direct sandwich ELISA system (catalog no. 10-1247-01, Mouse Insulin ELISA, Mercodia, Uppsala, Sweden) according to the manufacturer's protocol. LPS content was measured by using a fluorescence excitation/emission ELISA system (Pyrogene Recombinant Factor C Endotoxin Detection Assay, 50 to 658 U, Lonza, Visp, Switzerland) in serum diluted 1:1000, as established by using the product inhibition test according to the manufacturer's protocol. The diluted samples were heat-inactivated in 70 °C water bath for 10 min before proceeding, as recommended by the manufacturer. The fluorescence is proportional to the endotoxin concentration

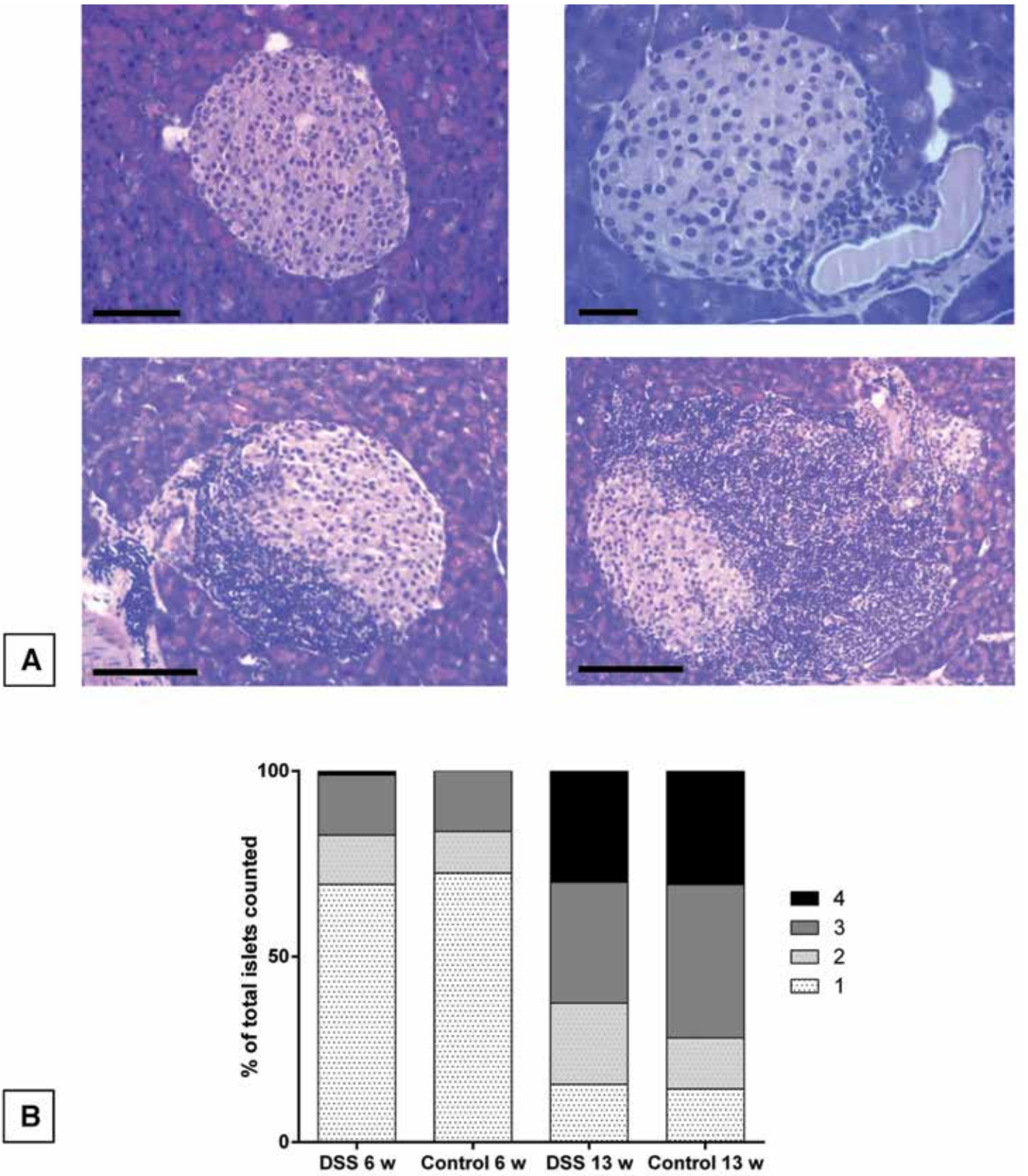

Figure 1. Insulitis evaluation. Insulitis of NOD mice treated with 1% DSS at weaning for 7 d was evaluated at weeks 6 and 13 and compared with that of control mice. (A) Islets of Langerhans with increasing infiltration. Representative histologic images of islet scores 1 through 4 used to evaluate insulitis. Upper left: score 1 = no infiltration (bar; 50 µm), upper right: score 2 = non-invasive peri-insulitis (bar; 20 µm), lower left: score 3 = invasive infiltration of <50% of islet (bar; 100 µm), and lower right: score 4 = invasive infiltration of >50% of islet (bar; 100 µm). (B) Overview of insulitis scores per group. The graph shows the assigned scores within treated and control groups (percentage of total number of counted islets per group).

Table 1. Insulitis scores (% of 20 islets per mouse; mean ± 1 SD) of NOD mice treated with 1% DSS for 7 d after weaning and of untreated control mice

	Score			
	1	2	3	4
Week 6				
DSS (n = 9)	69.4 ± 15.7	13.3 ± 6.6	16.1 ± 10.2	1.1 ± 2.2
Control (n = 8)	72.5 ± 19.1	11.3 ± 7.4	16.3 ± 14.6	0 ± 0
Week 13				
DSS (n = 8)	15.6 ± 11.5	21.9 ± 10.3	32.5 ± 8.5	30.0 ± 14.9
Control (n = 8)	14.4 ± 15.0	13.8 ± 10.3	41.3 ± 14.6	30.6 ± 18.9

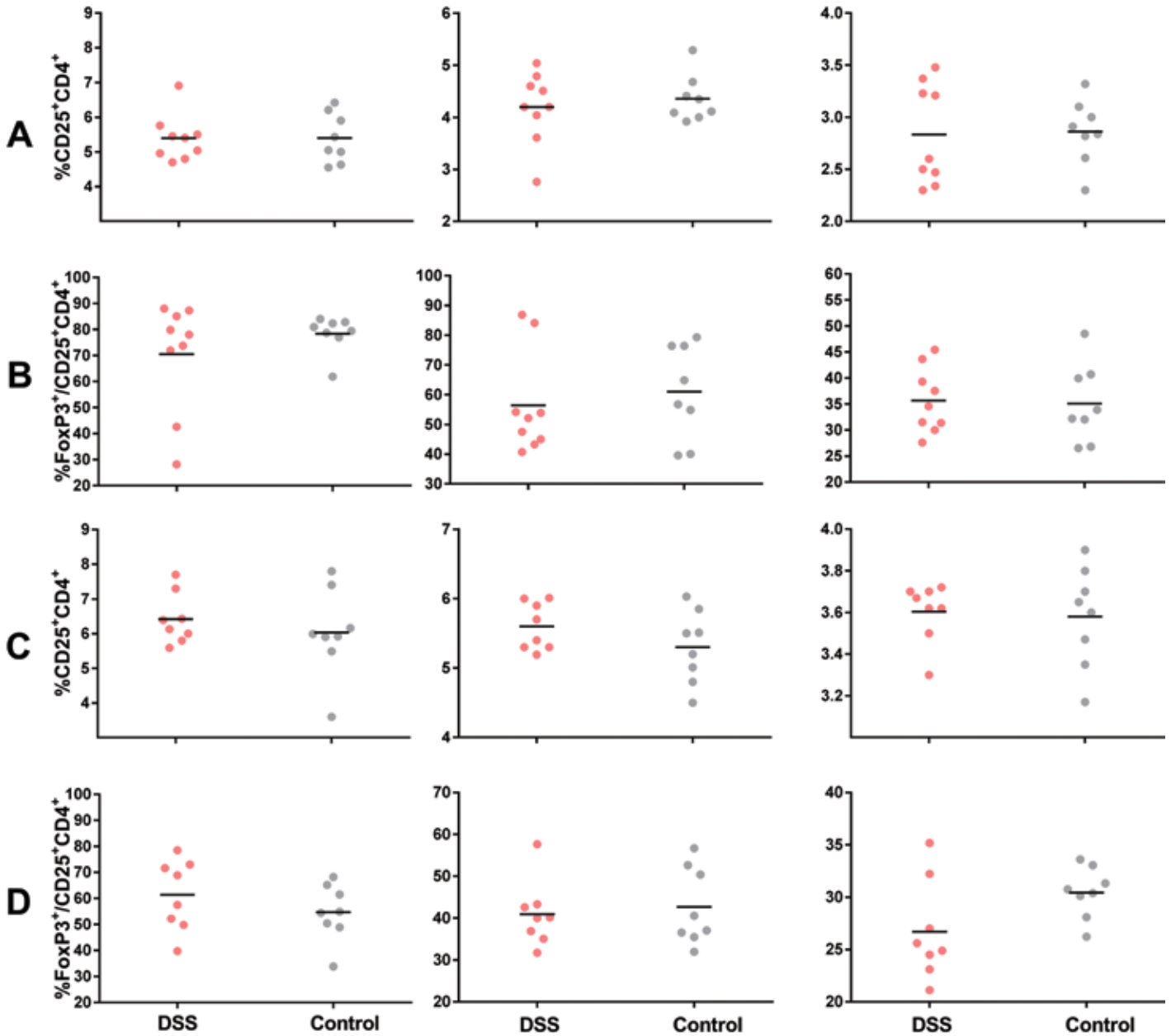

Figure 2. Flow cytometric evaluation of activated T and T_{reg} cells. Immune cell counts were evaluated in NOD mice treated with 1% DSS for 7 d, beginning at weaning, in pancreatic lymph nodes (left panels), mesenteric lymph nodes (middle panels), and spleen (right panels) at weeks 6 and 13. Horizontal lines indicate mean values. (A) Percentage of $CD25^+CD4^+$ cells at 6 wk. (B) Percentage of $FoxP3^+CD25^+CD4^+$ cells (T_{reg}) at 6 wk. (C) Percentage of $CD25^+CD4^+$ cells at 13 wk. (D) Percentage of $FoxP3^+$ $CD25^+CD4^+$ cells (T_{reg}) at 13 wk. No significant differences were found for any population.

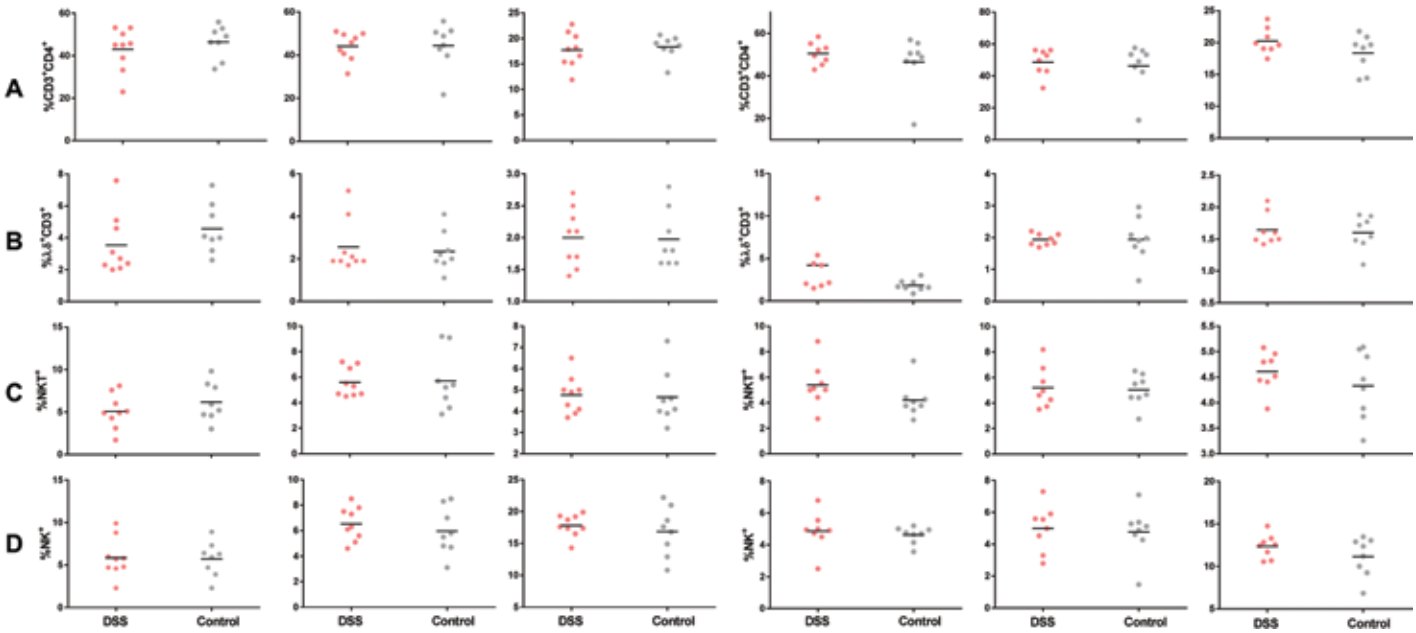

Figure 3. Flow cytometric evaluation of $CD3^+$, $\gamma\delta^+$, NK, and NKT cells at weeks 6 (3 leftmost columns of graphs) and 13 (3 rightmost columns of graphs) in pancreatic lymph nodes (left graph of each set of 3), mesenteric lymph nodes (middle), and spleen (right). Horizontal lines indicate mean values. (A) Percentages of $CD3^+CD4^+$ cells. (B) Percentages of $\gamma\delta^+CD3^+$ cells. (C) Percentages of NKT cells. (D) Percentages of NK cells. No significant differences were found for any population.

Table 2. Age (d) of control and DSS-treated NOD mice at disease onset and blood glucose concentration at euthanasia

		Control	DSS
Age (d) when blood glucose >7 mmol/L	*n*	17	11
	Mean	158.9	150.5
	1 SD	35.24	33.97
	Minimum	105	84
	Maximum	217	187
Age (d) when blood glucose ≥12 mmol/L	*n*	16	18
	Mean	164.6	159.6
	1 SD	31.75	40.46
	Minimum	105	84
	Maximum	224	231
Blood glucose (mmol/L) at euthanasia	*n*	15	17
	Mean	16.34	17.9
	1 SD	4.04	2.48
	Minimum	12.20	12.7
	Maximum	27.8	22.10

NOD mice were treated with 1% DSS for 7 d, beginning at weaning. Blood glucose of untreated control and DSS-treated mice was monitored at least weekly beginning 10 wk of age. Mice were considered hyperglycemic when blood glucose exceeded 7 mmol/L and monitored twice weekly; once the blood glucose exceeded 12 mmol/L for 2 consecutive measurements, the mice were diagnosed as diabetic and euthanized.

on a double-log scale and is linear in the range of 0.005 to 5.0 endotoxin units.

Histology. For scoring of insulitis, mice were killed by cervical dislocation and the pancreas placed in formaldehyde until embedded in paraffin and stained with hematoxylin and eosin. Scores were given to each of 25 islets per mouse across 6 slides. Scores were assigned as: 1, no to slight mononuclear cell infiltration at the edges of the islet; 2, less than 25% of the islet affected; 3, 25% to 50% affected; 4, more than 50% affected (Figure 1 A). For histologic evaluation, the gut was exteriorized, and the colon (from cecum to distal colon, without anus) and ileum (2.5 cm) were opened longitudinally. The surface was cleaned and flushed with cold PBS, and the tissue was rolled transversally with the luminal surface inside. The rolls were fixed by using a 27-gauge

needle, preserved in formaldehyde for 5 d, and then placed in 70% ethanol until paraffin embedding.

Bacterial DNA. When mice were handled, fecal pellets were collected in sterile microtubes and stored at –80 °C until bacterial DNA was extracted (catalog no. 51504, QIAamp DNA Stool Mini Kit, Qiagen, Hilden, Germany). The quality and quantity of DNA were assessed (NanoDrop 1000, Thermo Scientific, Waltham, MA) before storage at –80 °C. Samples were purified (PowerClean Pro DNA Clean-Up Kit, Mo Bio Laboratories, Carlsbad, CA), and spermine was added to prevent DSS from inhibiting the polymerase.

High-throughput sequencing. The composition of the fecal microbiota was determined by using tag-encoded 16S rRNA high-throughput sequencing (MiSEquation 2 × 250PE, Illumina). Cellular DNA extraction, DNA storage, sequencing library preparation steps, and merging and trimming of the raw dataset containing pair-ended reads with corresponding quality scores were done as previously described.[30] For analysis steps, the Quantitative Insight Into Microbial Ecology (QIIME) open-source software package[7] (versions 1.7.0 and 1.8.0) was used. The UPARSE pipeline[13] was used to purge chimeric reads from the data set and construct de novo operational taxonomic units (OTU). The Green Genes (version 13.8) 16S rRNA collection was used as a reference database.[24]

Principal coordinate analysis plots were generated by using the Jackknifed Beta Diversity workflow based on 10 distance metrics calculated by using 10 subsampled OTU tables. The number of sequences taken for each jackknifed subset was set to 85% of the sequence number within the most indigent sample. Weighted and unweighted UniFrac[20] distance matrices were generated based on rarefied (7500 reads per sample) OTU tables, and separation between the groups was tested with analysis of similarities (ANOSIM). The relative distribution of the registered genera was calculated for normalised and summarized at the genus level OTU tables.

The α diversity measures expressed for an observed species (sequence similarity, 97% OTU) value were computed for rarefied OTU tables (7500 reads per sample) using the α rarefaction workflow (QIMME v1.8.0). Differences in α diversity were determined by using a *t* test-based approach according to the nonparametric (Monte Carlo) method (999 permutations) implemented in the Compare α Diversity workflow (QIMME v1.8.0).

ANOVA was used to determine quantitative (relative abundance) association of OTUs with given group. These were calculated based on 1000 subsampled OTU tables rarefied to an equal number of reads (7500 per sample) and summarized to the genus level. Both the *P* value and the conservative FDR-corrected *P* value for multiple comparisons are reported.

The G test of independence (q_test) and ANOVA were used to determine qualitative (presence or absence) and quantitative (relative abundance) association of OTU with a given group, respectively. These were calculated based on 1000 subsampled OTU tables rarefied to an equal number of reads (7500).

Data were tested with the D'Agostino and Pearson omnibus normality test (Prism 6, GraphPad Software, San Diego, CA), and normally distributed data were tested at a 95% confidence level, with one-way ANOVA and paired or unpaired Student *t* tests with Welch correction for unequal variances, when appropriate. Nonparametric and small-sample–size data were tested with Kruskal–Wallis and the Wilcoxon matched-pairs test or Mann–Whitney test, where appropriate. For plasma insulin, outliers were detected and removed by using the ROUT method.[25] A general linear model was calculated for immune cells, with treatment as the primary factor and lymphatic organ as a secondary factor (Minitab 17, Coventry, United Kingdom).

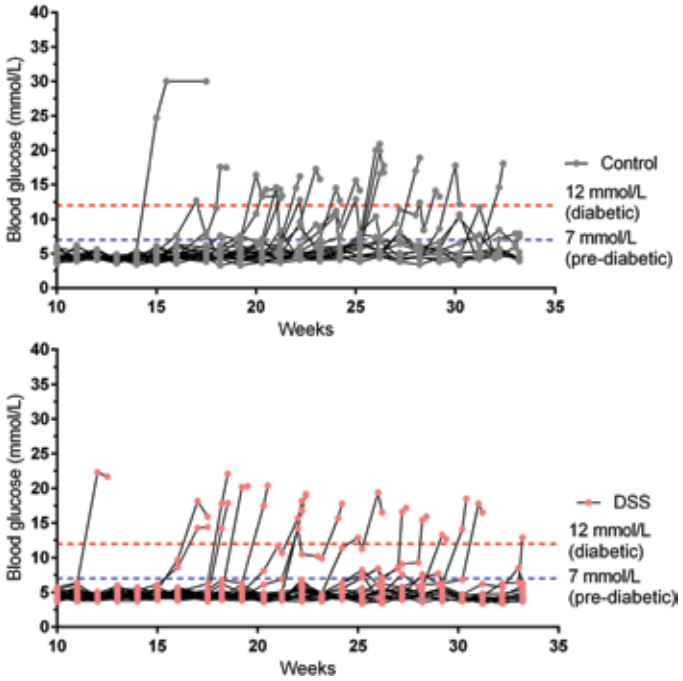

Figure 4. Blood glucose levels in control and DSS-treated NOD mice during weeks 10 through 33. Mice were monitored once each week from 10 wk of age and were considered hyperglycemic when blood glucose exceeded 7 mmol/L; they subsequently were monitored twice weekly until blood glucose exceeded 12 mmol/L on 2 consecutive measurements.

Results

Insulitis. Insulitis was evaluated in NOD mice at weeks 6 and 13 (Figure 1 and Table 1) and varied widely in both groups. When scores were grouped together as noninvasive (scores 1 and 2) and invasive (3 and 4), a mean of 72% of control group islets were invasively infiltrated compared with 62% of islets in DSS-treated mice (control median, 75%; DSS median, 70%; Mann–Whitney test for nonnormality, $P = 0.074$). No significant differences were found.

Immune cells. Flow cytometry was used to evaluate immune cells in the pancreatic lymph nodes, mesenteric lymph nodes, and spleen at weeks 6 and 13. Evaluation of activated T cells(Figure 2 A and C), T_{reg} cells (Figure 2 B and D), $CD3^+$ (Figure 3 A), $\gamma\delta^+$ (Figure 3 B), NKT (Figure 3 C), and NK (Figure 3 D) cells did not show significant differences for any population.

In addition, both $CD4^+$ and $FoxP3^+$ cell fractions were compared in general linear models, with treatment as the primary factor and lymphatic organ as a secondary factor. Neither $CD4^+$ nor $FoxP3^+$ cells differed in relation to treatment, whereas there were significant ($P = 0.000$) differences relative to which lymphatic organ they were sampled from.

Insulin, LPS, incidence, and blood glucose. Log-rank testing revealed no significant difference between the incidence curves. The median survival (defined as the time point at which 50%

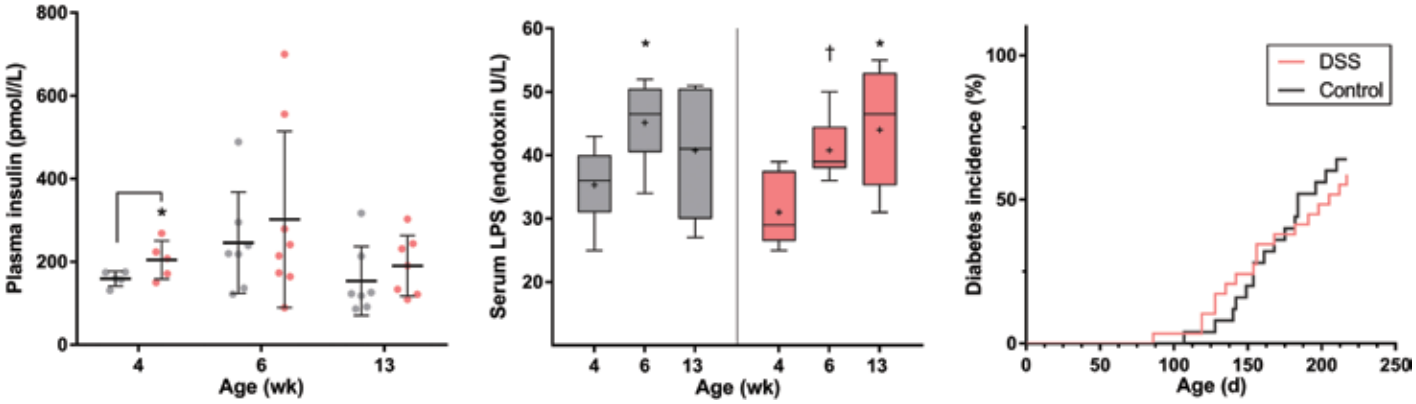

Figure 5. Insulin, LPS, and incidence. Plasma insulin and serum LPS values in control and DSS-treated NOD mice were measured at 4, 6, and 13 wk of age. Incidence was evaluated according to blood glucose measurements from week 10. Left: Plasma insulin (pmol/L; *, $P < 0.05$, unpaired t test with Welch correction for unequal variances). Middle: Box and whiskers plot of serum LPS (endotoxin U/mL; whiskers, minimum to maximum; line, median; +, mean). *, $P < 0.05$; †, $P < 0.01$ (unpaired t test). Right: Kaplan–Meier survival curve. Incidence is depicted as the proportion (%) of mice surviving relative to the total number of mice per group. Median survival (defined as the time point at which 50% of the mice are still alive) of the control group was 184 d compared with 205 d for DSS-treated mice.

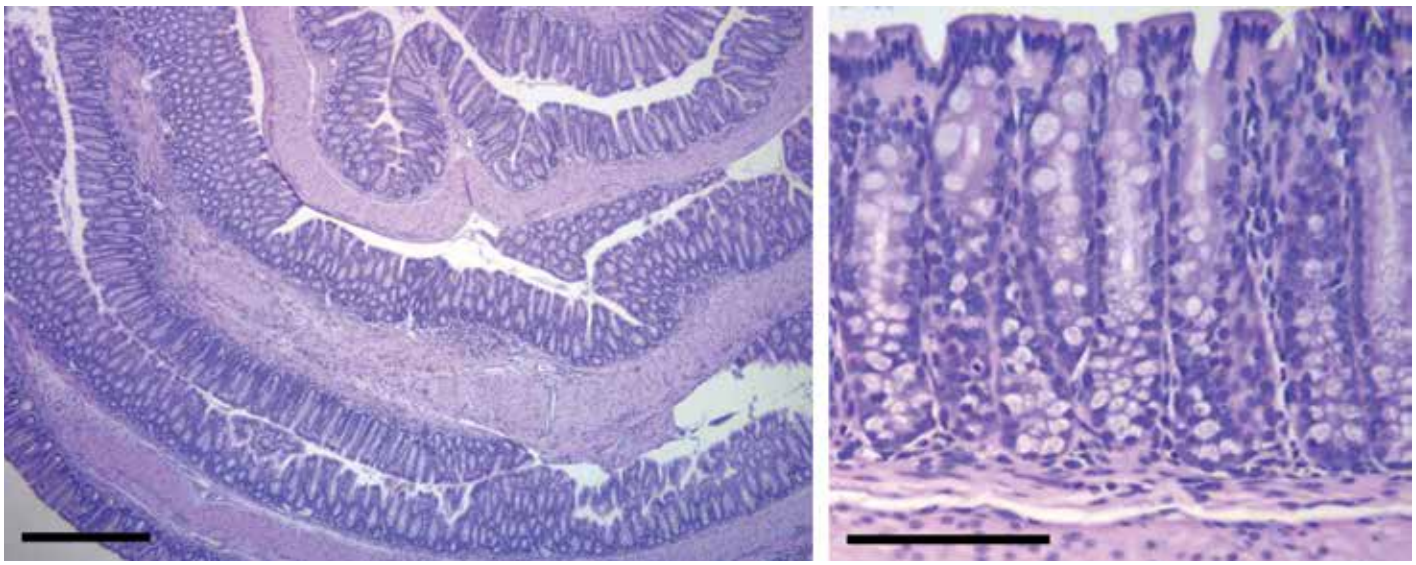

Figure 6. Histologic images of colon. Left: 'Swiss roll' of DSS-treated colon. Bar, 200 µm. Right: Normal colonic tissue from control animal. Bar, 50 µm. No pathologic changes were found upon histologic evaluation of control or DSS-treated NOD mice.

of the mice are still alive) was 184 d for the control group compared with 205 d for DSS-treated NOD mice. In addition, 15 of 24 (62.5%) mice in the control group reached a blood glucose level of 12 mmol/L before 30 wk, compared with 17 of 29 (59%) DSS-treated mice, with average ages at onset of 164 and 159 d, respectively (Table 2 and Figure 4). There was a transient effect on plasma insulin in week 4, immediately after DSS treatment, with a higher level in DSS mice than in control mice. Serum LPS did not differ between control and DSS, but increased from week 4 to 6 in both groups; subsequent values continued to increase in the DSS-treated mice but stabilized in control mice (Figure 5).

Cecum, colon, and gut microbiota. As expected, low-dose DSS treatment was not associated with histologic abnormalities on examination of the gut (Figure 6). DSS treatment significantly increased cecum length at all measured time points. DSS treatment tended to increase cecum weight in week 4 and 6, and the effect was significant in week 13. The effect of DSS on colon length approached significance in week 13 ($P = 0.072$; Figure 7).

Gut microbiota. In light of the change in cecum size, which also occurs in germ-free conditions, we investigated the effect of low-dose DSS treatment in early life on the gut microbiota composition. At early ages (weeks 4 and 6 combined), we found a general separation in principal coordinate analysis, based on unweighted UniFrac distance matrices (qualitative) between control and DSS-treated mice (Figure 8). Because weighted UniFrac distance matrices (quantitative) showed no clear clustering, the difference in microbial composition between week 4 and 6 is mainly due to the low-abundance or distantly related taxa. Evaluation of the presence and absence of bacteria (G test) showed that 10 OTU classified to the Lachnospiraceae family (Firmicutes) and 2 OTU from S24-7 (Bacteriodetes) were significantly ($P < 0.01$) underrepresented in the DSS group in weeks 4 and 6 (Table 3). In week

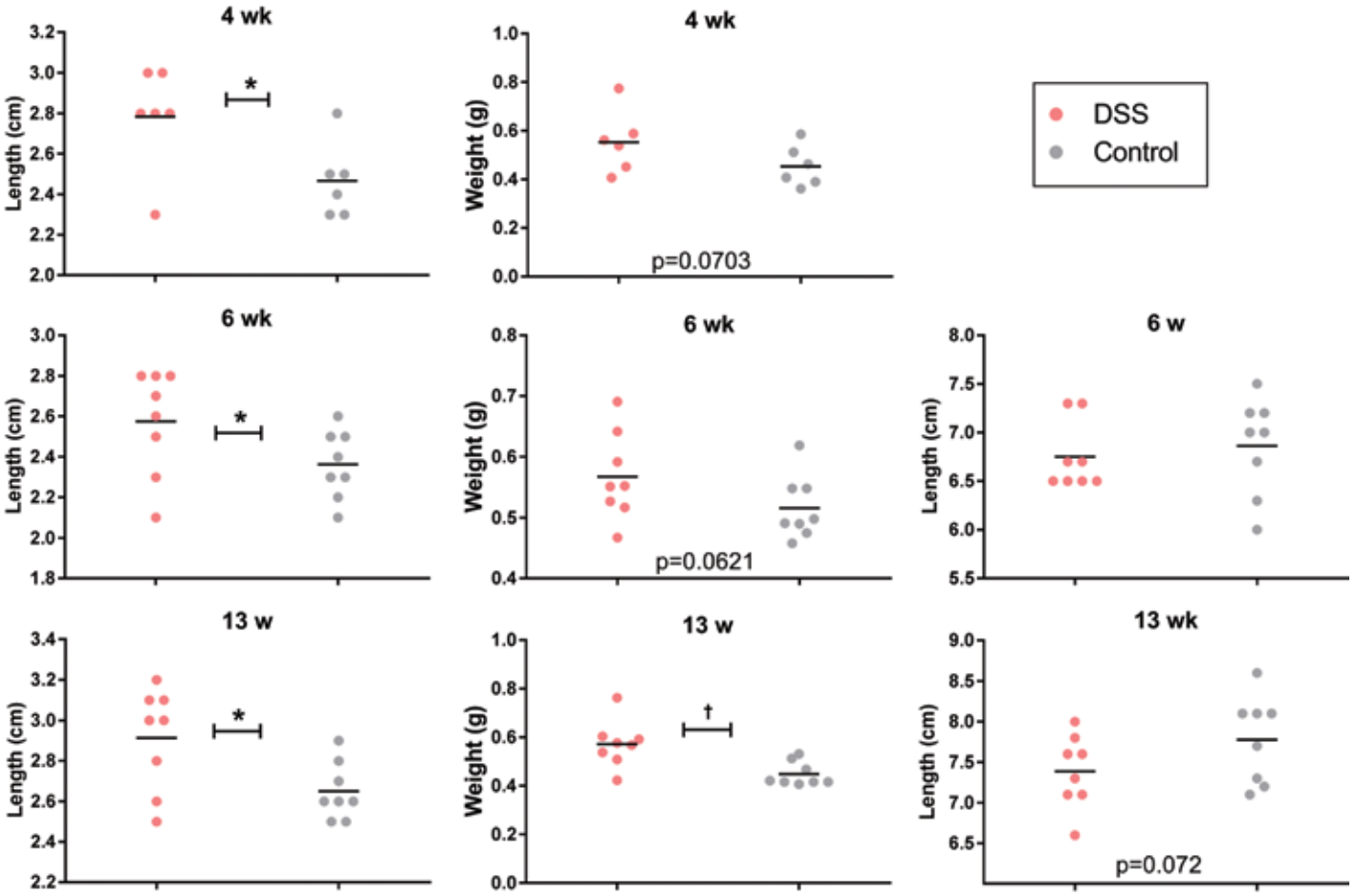

Figure 7. Cecal length (left panels) and weight (middle panels) and colonic length (right panels) measured after euthanasia of control and DSS-treated NOD mice at 4, 6, and 13 wk of age. Horizontal lines indicate mean values. *, $P < 0.05$; †, $P < 0.01$ (unpaired t test).

13, 6 members of the Rikenellaceae family from the Bacteroidetes phylum were significantly ($P < 0.01$) underrepresented, and DSS likely affected the presence of these bacteria. However, relative abundancy of taxa did not differ between DSS-treated and control NOD mice at week 4, 6, or 13 (Figure 9).

Discussion

In this study, we tested whether a brief early-life intervention would influence disease development in NOD mice. NOD mice potentially are prediabetic beginning at week 3 of age, and some mice may already have developed diabetes at week 10. We evaluated the incidence of diabetes until 30 wk of age; insulitis, immune cells, and gut microbiota composition were evaluated at 6 and 13 wk.

The low-dose DSS treatment at weaning changed the composition of the gut microbiota transiently, influenced the gut metrics, and briefly differentiated plasma insulin levels at 4 wk. However, it had no significant influence on the numbers of immune cells, insulitis, or diabetes incidence, demonstrating the robustness of the NOD model despite early-life interruption of gut homeostasis, barrier function, and microbiota.

Insulitis scores in the current study were subject to large variation, which might have contributed to the nonsignificant result. In particular, although mean values suggested between-group differences (at 13 wk, 72% of control group islets were invasively infiltrated compared with 62% in DSS-treated mice), testing of median values yielded only a statistical tendency ($P = 0.074$, Mann–Whitney). In another study, the mice failed to develop a significant difference in insulitis until 20 wk, even though significant differences in microbiota, gastrointestinal pH, and FoxP3 expression were demonstrated from 2 wk of age.[34] These data further emphasize the robustness of the end-disease outcome of NOD mice.

The low-dose DSS treatment we used had some effect on the gut of NOD mice, demonstrated by the robust differences in cecal length and weight from week 4 through 13. Colonic shortening, a standard effect of colonic DSS treatment, was not significant at week 6; however, there was a tendency toward delayed shortening in the DSS-treated mice at week 13 despite the lack of changes in the histologic evaluation. A similar pattern was seen in the LPS data: in DSS-treated mice, serum LPS levels in continued to increase from 4 to 13 wk, whereas the control group remained at same level as in week 6. These data indicate that DSS treatment has a progressive effect on the gut barrier.

Diabetes incidence is the final outcome of the model, but the prediabetic changes are more interesting in terms of disease mechanisms. The cellular mechanisms in these early stages respond to changes in the homeostasis of the gut microbiota due to

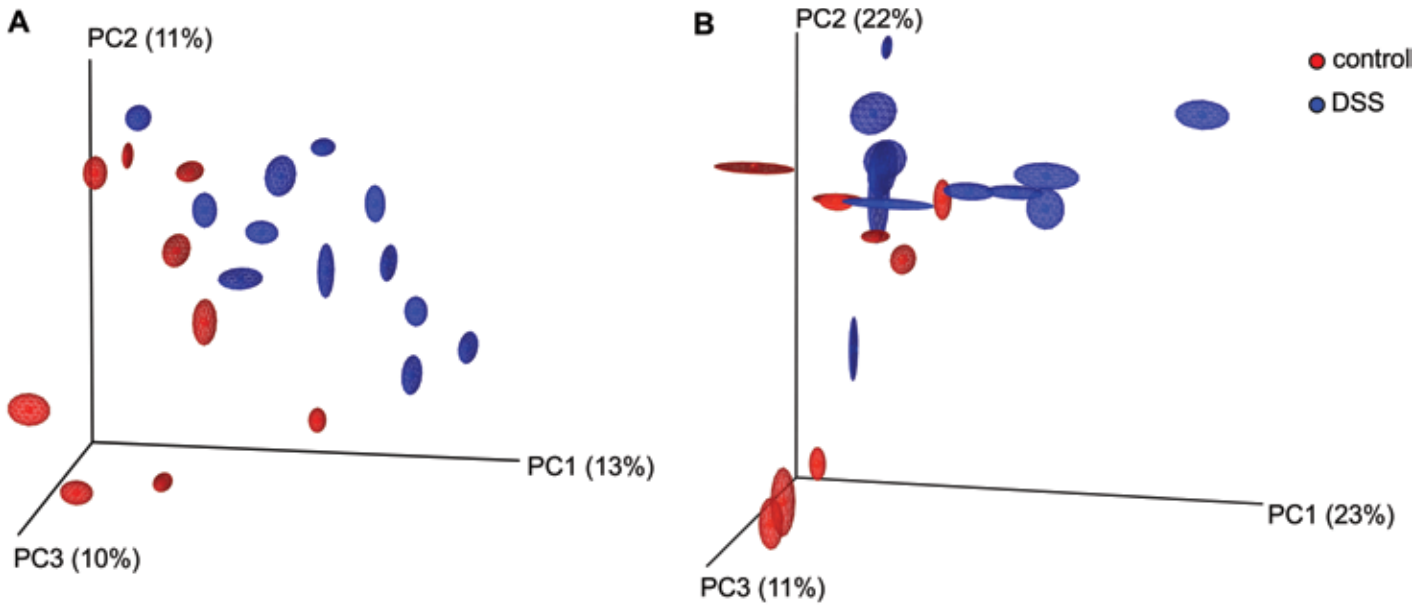

Figure 8. Plots of differences in gut microbiota composition. Fecal samples collected during weeks 4 and 6 (combined) from DSS-treated and untreated control NOD mice. Principal coordinate analysis plots are based on (A) unweighted and (B) generalized UniFrac distance matrices calculated from 10 rarefied (7500 reads per sample) OTU tables. PERMANOVA (F = 1.990, *P* = 0.001) and PERMANOVA-g (F = 1.827, *P* = 0.025) analyses based on unweighted and generalized UniFrac distance matrices, respectively, show significant separation between the 2 categories. The degree of variation between 10 jackknifed replicates of principal coordinate analysis is displayed with confidence ellipsoids around each sample. Weighted UniFrac analysis did not yield any separation between the categories (data not shown).

Table 3. Results of G test of independence

Phylum	Class	Order	Family	Genus	G probability per 1000 OTU tables	FDR corrected for 392 observations	OTU positive DSS	OTU positive Control	OTU negative. DSS	OTU negative Control
OTU (4 and 6 wk of age)										
Firmicutes	Clostridia	Clostridiales	Lachnospiraceae	—	0.001	0.381	0, 4	7, 3	12, 8	2, 6
Firmicutes	Clostridia	Clostridiales	Lachnospiraceae	—	0.004	0.857	0, 3	6, 3	12, 9	3, 6
Firmicutes	Clostridia	Clostridiales	Lachnospiraceae	—	0.009	1.153	4, 7	9, 6	8, 5	0, 3
Firmicutes	Clostridia	Clostridiales	Lachnospiraceae	—	0.009	0.916	2, 6	9, 5	10, 6	0, 4
Firmicutes	Clostridia	Clostridiales	Lachnospiraceae	—	0.021	1.640	2, 5	7, 4	10, 7	2, 5
Firmicutes	Clostridia	Clostridiales	Lachnospiraceae	—	0.027	1.527	5, 8	9, 6	7, 4	0, 3
Firmicutes	Clostridia	Clostridiales	Lachnospiraceae	—	0.035	1.720	4, 7	8, 5	8, 5	1, 4
Firmicutes	Clostridia	Clostridiales	Lachnospiraceae	—	0.036	1.573	2, 6	9, 5	10, 5	0, 4
Firmicutes	Clostridia	Clostridiales	Lachnospiraceae	—	0.038	1.482	5, 8	9, 6	7, 4	0, 3
Firmicutes	Clostridia	Clostridiales	Lachnospiraceae	—	0.048	1.698	2, 5	7, 4	10, 6	2, 5
Bacteroidetes	Bacteroidia	Bacteroidales	S24-7	—	0.026	1.680	1, 5	7, 3	11, 7	2, 5
OTU (13 wk of age)										
Bacteroidetes	Bacteroidia	Bacteroidales	Rikenellaceae	—	0.009	1.006	0, 3	6, 3	8, 5	1, 4
Bacteroidetes	Bacteroidia	Bacteroidales	Rikenellaceae	—	0.014	1.128	1, 4	6, 3	7, 4	1, 4
Bacteroidetes	Bacteroidia	Bacteroidales	Rikenellaceae	—	0.031	2.031	0, 3	5, 2	8, 5	2, 5
Bacteroidetes	Bacteroidia	Bacteroidales	Rikenellaceae	—	0.003	1.093	0, 3	6, 3	8, 5	1, 4
Bacteroidetes	Bacteroidia	Bacteroidales	Rikenellaceae	—	0.005	0.752	0, 3	6, 3	8, 5	1, 4
Bacteroidetes	Bacteroidia	Bacteroidales	Rikenellaceae	—	0.009	1.006	0, 3	6, 3	8, 5	1, 4

Fecal samples were collected during weeks 4, 6, and 13 from untreated control and DSS-treated NOD. Mice were treated with 1% DSS at weaning for 7days. The G test of independence (g_test) based on 1000 subsampled operational taxonomic unit (OUT) tables rarefied to the identical number of reads (7500 per sample) indicates whether the presence or absence of a species is associated with a given category. The false discovery rate (FDR) represents the probability after correction with FDR, where the raw *P* values are first ranked from low to high and then each *P* value is multiplied by the number of tests divided by this rank. The 2 numbers in the OTU_positive columns respectively represent the number of OTU observed within a given group and the number of OTU expected to be observed if the OTU was distributed randomly across samples from this category. The 2 numbers in the OTU_negative columns respectively represent the number of OTU missing within a given group and the number of OTU expected to be missed if the OTU was distributed randomly across samples from this category.

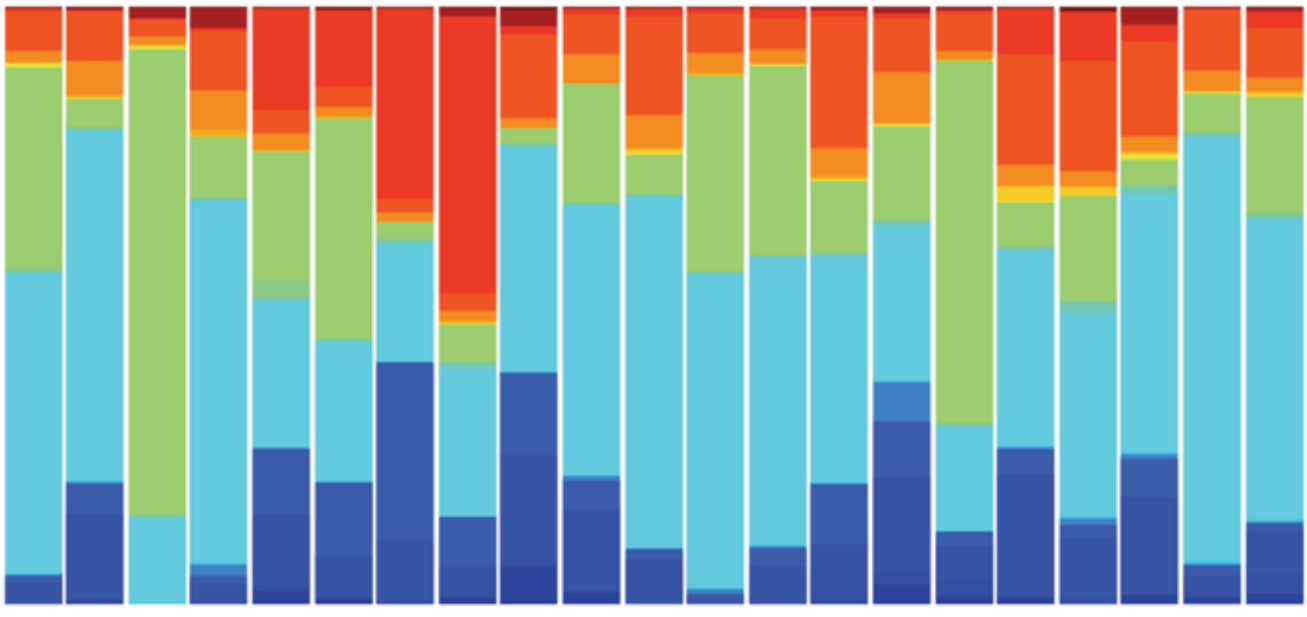

phylum	class	order	family	genus	species
Bacteroidetes	Bacteroidia	Bacteroidales	Other	Other	Other
Bacteroidetes	Bacteroidia	Bacteroidales	Bacteroidaceae	Bacteroides	Unclassified
Bacteroidetes	Bacteroidia	Bacteroidales	Bacteroidaceae	Bacteroides	uniformis
Bacteroidetes	Bacteroidia	Bacteroidales	Porphyromonadaceae	Parabacteroides	Unclassified
Bacteroidetes	Bacteroidia	Bacteroidales	Prevotellaceae	Prevotella	Unclassified
Bacteroidetes	Bacteroidia	Bacteroidales	Rikenellaceae	Unclassified	Unclassified
Bacteroidetes	Bacteroidia	Bacteroidales	S24-7	Unclassified	Unclassified
Cyanobacteria	Chloroplast	Streptophyta	Unclassified	Unclassified	Unclassified
Deferribacteres	Deferribacteres	Deferribacterales	Deferribacteraceae	Mucispirillum	schaedleri
Firmicutes	Bacilli	Lactobacillales	Lactobacillaceae	Lactobacillus	Unclassified
Firmicutes	Clostridia	Clostridiales	Other	Other	Other
Firmicutes	Clostridia	Clostridiales	Unclassified	Unclassified	Unclassified
Firmicutes	Clostridia	Clostridiales	Clostridiaceae	Unclassified	Unclassified
Firmicutes	Clostridia	Clostridiales	Clostridiaceae	CandidatusArthromitus	Unclassified
Firmicutes	Clostridia	Clostridiales	Dehalobacteriaceae	Dehalobacterium	Unclassified
Firmicutes	Clostridia	Clostridiales	Lachnospiraceae	Other	Other
Firmicutes	Clostridia	Clostridiales	Lachnospiraceae	Unclassified	Unclassified
Firmicutes	Clostridia	Clostridiales	Lachnospiraceae	Blautia	Unclassified
Firmicutes	Clostridia	Clostridiales	Lachnospiraceae	Butyrivibrio	Unclassified
Firmicutes	Clostridia	Clostridiales	Lachnospiraceae	Coprococcus	Unclassified
Firmicutes	Clostridia	Clostridiales	Lachnospiraceae	Dorea	Unclassified
Firmicutes	Clostridia	Clostridiales	Lachnospiraceae	[Ruminococcus]	gnavus
Firmicutes	Clostridia	Clostridiales	Ruminococcaceae	Other	Other
Firmicutes	Clostridia	Clostridiales	Ruminococcaceae	Unclassified	Unclassified
Firmicutes	Clostridia	Clostridiales	Ruminococcaceae	Anaerotruncus	Unclassified
Firmicutes	Clostridia	Clostridiales	Ruminococcaceae	Oscillospira	Unclassified
Firmicutes	Clostridia	Clostridiales	Ruminococcaceae	Ruminococcus	Unclassified
Firmicutes	Clostridia	Clostridiales	[Mogibacteriaceae]	Unclassified	Unclassified
Firmicutes	Erysipelotrichi	Erysipelotrichales	Erysipelotrichaceae	Unclassified	Unclassified
Proteobacteria	Alphaproteobacteria	Unclassified	Unclassified	Unclassified	Unclassified
Tenericutes	Mollicutes	Anaeroplasmatales	Anaeroplasmataceae	Anaeroplasma	Unclassified
Tenericutes	Mollicutes	RF39	Unclassified	Unclassified	Unclassified
Other					

Figure 9. Abundance of various gut bacteria. Fecal samples were collected during weeks 4 and 6 (combined) and week 13 from DSS-treated and untreated control NOD mice. ANOVA identified no significant differences.

particular food elements, antibiotics, and other factors and likely are critical for future disease development within an individual. The pattern of fluctuations in the blood glucose concentration, for instance, has been proposed to reflect 2 phenotypes: one in which the concentration progressively and steadily rises and the other in which blood glucose acutely increases. Mice with lower starting blood glucose values and steady rise were associated with higher disease reversal.[22] In our study, plasma insulin showed a transient significant difference at 4 wk of age, indicating an acute but not persistent effect of DSS treatment. This finding could be a result of the temporarily increased permeability across the barrier, with increased uptake leading to transiently increased insulin level.

The low dose of DSS in the current study did not have any marked effect on the standard disease parameters of the NOD model. Because this model is considered highly dependent on environmental influences, the idea of using a simple gut intervention early in life to induce oral tolerance and decrease disease expression is attractive. Data from our laboratory show that DSS changes the composition of the gut microbiota, characterized by increases in gram-negative strains, such as Proteobacteria, and decreases in Firmicutes, and an overall decrease in diversity.[4] Similar tendencies were seen in the current study, where Rikenellaceae and Lachnospiraceae were underrepresented in the DSS group at weeks 4 and 6.

The importance of the microbiota in the NOD mouse is unquestionable,[29] but whether the microbiota is a disease factor to be manipulated or a result of stable intrinsic genetic conditions and the contributions of the diet in these scenarios remain unresolved. Some have suggested that NOD mice already have a 'diabetogenic' microbiota.[5] One study found fewer colonic Alphaproteobacteria, *Bacteroides*, and Ruminococcus and the presence of Prevotella, generally concluding that NOD mice contained more pathogenic strains and an overall different metabolic profile, compared with diabetes-resistant mice.[5] In that study, after fecal transplantation of NOD microbiota to diabetes-resistant mice, the normally limited insulitis of the diabetes-resistant mice was exacerbated. Interestingly, fecal transplantation of microbiota from diabetes-resistant mice to NOD recipients did not overcome their diabetes. In turn, administration of the probiotic VSL3 did not achieve any effective colonization or disease amelioration.[5]

Interventions achieving most profound effects on diabetes development occur during fetal life, by targeting the mother, for example, through gluten-free diets or antibiotic treatment. Conflicting results have been reported for vancomycin, depending on treatment timing: one study reported decreased incidence and increased *Akkermansia* and tolerance when administered until weaning of NOD mice,[17] suggesting a health-improving effect on the already established microbiota. In another report, administration of vancomycin to NOD mice from fetal life until the end of the study increased disease incidence, *Akkermansia* species, and Th1-type cells, pointing to a different microbiotal starting point as well as a difference between brief early-life manipulation and prolonged microbiotal intervention.[5] Very early-life events that affect the establishment of the (diabetogenic) microbiota clearly seem to be important for disease development in the NOD model.

DSS is known to disrupt the gut barrier, and we hypothesized that this early-life intervention would increase the tolerogenic effects of antigen–host contact, which normally leads to oral tolerance and T_{reg} induction. However, NOD mice may have deficiencies in antigen-presenting dendritic cells.[27] In addition, although the DSS treatment we used was low-dose and brief, NOD mice may have a leaky gut, which has been proposed as a disease mechanism[5,33] leading to an increased Th1 inflammatory setting.

In conclusion, under the study conditions, DSS-induced disruption of small intestinal barrier function early in life failed to influence immune cells and did not overcome the disease mechanisms of the NOD mouse model. Other interventions, perhaps occurring much earlier in life, seem to be necessary to overrule the robustness of the NOD model.

Acknowledgments

The study was sponsored by the Novo Nordisk Life In Vivo Pharmacology Centre and by the Gut, Grain, and Greens program of the Danish Innovation Fund. We thank Kirsten Reichwald for assistance with flow cytometry.

References

1. **Atarashi K, Tanoue T, Shima T, Imaoka A, Kuwahara T, Momose Y, Cheng G, Yamasaki S, Saito T, Ohba Y, Taniguchi T, Takeda K, Hori S, Ivanov II, Umesaki Y, Itoh K, Honda K.** 2011. Induction of colonic regulatory T cells by indigenous *Clostridium* species. Science **331:**337–341.
2. **Bangsgaard Bendtsen KM, Krych L, Sørensen DB, Pang W, Nielsen DS, Josefsen K, Hansen LH, Sørensen SJ, Hansen AK.** 2012. Gut microbiota composition is correlated to grid floor induced stress and behavior in the BALB/c mouse. PLoS One **7:**1–10.
3. **Bendtsen KM, Fisker L, Hansen AK, Hansen CH, Nielsen DS.** 2015. The influence of the young microbiome on inflammatory diseases—lessons from animal studies. Birth Defects Res C Embryo Today **105:**278–295.
4. **Bendtsen KM, Hansen CHF, Krych Ł, Skovgaard K, Kot W,Vogensen FK,Hansen AK.** 2017. Immunological effects of reduced mucosal integrity in the early life of BALB/c mice. PLoS One **12:**1–20.
5. **Brown K, Godovannyi A, Ma C, Zhang Y, Ahmadi-Vand Z, Dai C, Gorzelak MA, Chan Y, Chan JM, Lochner A, Dutz JP, Vallance BA, Gibson DL.** 2015. Prolonged antibiotic treatment induces a diabetogenic intestinal microbiome that accelerates diabetes in NOD mice. ISME J **10:**321–332.
6. **Calcinaro F, Dionisi S, Marinaro M, Candeloro P, Bonato V, Marzotti S, Corneli RB, Ferretti E, Gulino A, Grasso F, De Simone C, Di Mario U, Falorni A, Boirivant M, Dotta F.** 2005. Oral probiotic administration induces interleukin-10 production and prevents spontaneous autoimmune diabetes in the nonobese diabetic mouse. Diabetologia **48:**1565–1575.
7. **Caporaso JG, Kuczynski J, Stombaugh J, Bittinger K, Bushman FD, Costello EK, Fierer N, Gonzalez Pena A, Goodrich JK, Gordon JI, Huttley GA, Kelley ST, Knights D, Koenig JE, Ley RE, Lozupone CA, McDonald D, Muegge BD, Pirrung M, Reeder J, Sevinsky JR, Turnbaugh PJ, Walters WA, Widmann J, Yatsunenko T, Zaneveld J, Knight R.** 2010 QIIME allows analysis of high-throughput community sequencing data. Nat Methods **7:**335–336.
8. **Cardell SL.** 2006. The natural killer T lymphocyte: a player in the complex regulation of autoimmune diabetes in non-obese diabetic mice. Clin Exp Immunol **143:**194–202.
9. **Chistiakov DA, Bobryshev YV, Kozarov E, Sobenin IA, Orekhov AN.** 2015. Intestinal mucosal tolerance and impact of gut microbiota to mucosal tolerance. Front Microbiol **5:**781.
10. **Clemente-Casares X, Blanco J, Ambalavanan P, Yamanouchi J, Singha S, Fandos C, Tsai S, Wang J, Garabatos N, Izquierdo C, Agrawal S, Keough MB, Yong VW, James E, Moore A, Yang Y, Stratmann T, Serra P, Santamaria P.** 2016. Expanding antigen-specific regulatory networks to treat autoimmunity. Nature **530:**434–440.
11. **Delovitch TL, Singh B.** 1997. The nonobese diabetic mouse as a model of autoimmune diabetes: immune dysregulation gets the NOD. Immunity **7:**727–738.

12. **De Fazio L, Cavazza E, Spisni E, Strillacci A, Centanni M, Candela M, Praticò C, Campieri M, Ricci C, Valerii MC.** 2014. Longitudinal analysis of inflammation and microbiota dynamics in a model of mild chronic dextran sulfate sodium-induced colitis in mice. World J Gastroenterol **20:**2051–2061.
13. **Edgar RC.** 2013. UPARSE: highly accurate OTU sequences from microbial amplicon reads. Nat Methods **10:** 996–998.
14. **FELASA working group on revision of guidelines for health monitoring of rodents and rabbits, Mähler Convenor M**, **Berard M**, **Feinstein R**, **Gallagher A**, **Illgen-Wilcke B**, **Pritchett-Corning K**, **Raspa M**. 2014. FELASA recommendations for the health monitoring of mouse, rat, hamster, guinea pig, and rabbit colonies in breeding and experimental units. Lab Anim **48:**178–192.
15. **Geuking MB, Cahenzli J, Lawson MA, Ng DC, Slack E, Hapfelmeier S, McCoy KD, Macpherson AJ.** 2011. Intestinal bacterial colonization induces mutualistic regulatory T cell responses. Immunity **34:**794–806.
16. **Hansen CH, Krych L, Buschard K, Metzdorff SB, Nellemann C, Hansen LH, Nielsen DS, Frøkiær H, Skov S, Hansen AK.** 2014. A maternal gluten-free diet reduces inflammation and diabetes incidence in the offspring of NOD mice. Diabetes **63:**2821–2832.
17. **Hansen CH, Krych L, Nielsen DS, Vogensen FK, Hansen LH, Sørensen SJ, Buschard K, Hansen AK.** 2012. Early life treatment with vancomycin propagates *Akkermansia muciniphila* and reduces diabetes incidence in the NOD mouse. Diabetologia **55:**2285–2294.
18. **Johansson ME, Gustafsson JK, Sjöberg KE, Petersson J, Holm L, Sjövall H, Hansson GC.** 2010. Bacteria penetrate the inner mucus layer before inflammation in the dextran sulfate colitis model. PLoS One **5:**1–9.
19. **Kriegel MA, Sefik E, Hill JA, Wu HJ, Benoist C, Mathis D.** 2011. Naturally transmitted segmented filamentous bacteria segregate with diabetes protection in nonobese diabetic mice. Proc Natl Acad Sci USA **108:**11548–11553.
20. **Lozupone C**, **Lladser ME**, **Knights D**, **Stombaugh J**, **Knight R.** 2011 UniFrac: an effective distance metric for microbial community comparison. ISME J **5:**169–172.
21. **Marietta EV, Gomez AM, Yeoman C, Tilahun AY, Clark CR, Luckey DH, Murray JA, White BA, Kudva YC, Rajagopalan G.** 2013. Low incidence of spontaneous type 1 diabetes in nonobese diabetic mice raised on gluten-free diets is associated with changes in the intestinal microbiome. PLoS One **8:**1–9.
22. **Mathews CE, Xue S, Posgai A, Lightfoot YL, Li X, Lin A, Wasserfall C, Haller MJ, Schatz D, Atkinson MA.** 2015. Acute versus progressive onset of diabetes in nod mice: potential implications for therapeutic interventions in type 1 diabetes. Diabetes **64:**3885–3890.
23. **Mazmanian SK.** 2009. Gut immune balance is as easy as S-F-B. Immunity **31:**536–538.
24. **McDonald D**, **Price MN**, **Goodrich J**, **Nawrocki EP**, **DeSantis TZ**, **Probst A**, **Andersen GL**, **Knight R**, **Hugenholtz P**. 2012 An improved GreenGenes taxonomy with explicit ranks for ecological and evolutionary analyses of bacteria and archaea. ISME J **6:**610–618.
25. **Motulsky HJ, Brown RE.** 2006. Detecting outliers when fitting data with nonlinear regression—a new method based on robust nonlinear regression and the false discovery rate. BMC Bioinformatics **7:**1–20.
26. **Nielsen DS, Krych L, Buschard K, Hansen CH, Hansen AK.** 2014. Beyond genetics: influence of dietary factors and gut microbiota on type 1 diabetes. FEBS Lett **588:**4234–4243.
27. **O'Keeffe M, Brodnicki TC, Fancke B, Vremec D, Morahan G, Maraskovsky E, Steptoe R, Harrison LC, Shortman K.** 2005. FMS-like tyrosine kinase 3 ligand administration overcomes a genetically determined dendritic cell deficiency in NOD mice and protects against diabetes development. Int Immunol **17:**307–314.
28. **Okayasu I, Hatakeyama S, Yamada M, Ohkusa T, Inagaki Y, Nakaya R**. 1990. A novel method in the induction of reliable experimental acute and chronic ulcerative-colitis in mice. Gastroenterology **98**:694–702.
29. **Pearson JA, Wong FS, Wen L.** 2016. The importance of the nonobese diabetic (NOD) mouse model in autoimmune diabetes. J Autoimmun **66:**76–88.
30. **Pyndt Jørgensen B, Hansen JT, Krych L, Larsen C, Klein AB, Nielsen DS, Josefsen K, Hansen AK, Sørensen DB.** 2014. A possible link between food and mood: dietary impact on gut microbiota and behavior in BALB/c mice. PLoS One **9:**1–15.
31. **Schwab C, Berry D, Rauch I, Rennisch I, Ramesmayer J, Hainzl E, Heider S, Decker T, Kenner L, Müller M, Strobl B, Wagner M, Schleper C, Loy A, Urich T.** 2014. Longitudinal study of murine microbiota activity and interactions with the host during acute inflammation and recovery. ISME J **8:**1101–1114.
32. **Sildorf SM, Fredheim S, Svensson J, Buschard K**. 2012.Remission without insulin therapy on gluten-free diet in a 6-y old boy with type 1 diabetes mellitus. BMJ Case Reports.
33. **Vaarala O, Atkinson MA, Neu J.** 2008. The 'perfect storm' for type 1 diabetes: the complex interplay between intestinal microbiota, gut permeability, and mucosal immunity. Diabetes **57:**2555–2562.
34. **Wolf KJ, Daft JG, Tanner SM, Hartmann R, Khafipour E, Lorenz RG.** 2014. Consumption of acidic water alters the gut microbiome and decreases the risk of diabetes in NOD mice. J Histochem Cytochem **62:**237–250.